

Characteristic magnetic field and speed properties of interplanetary coronal mass ejections and their sheath regions

M. J. Owens

Center for Space Physics, Boston University, Boston, Massachusetts, USA

P. J. Cargill

Space and Atmospheric Physics, The Blackett Laboratory, Imperial College, London, UK

C. Pagel, G. L. Siscoe, and N. U. Crooker

Center for Space Physics, Boston University, Boston, Massachusetts, USA

Received 30 September 2004; revised 8 November 2004; accepted 16 November 2004; published 20 January 2005.

[1] Prediction of the solar wind conditions in near-Earth space, arising from both quasi-steady and transient structures, is essential for space weather forecasting. To achieve forecast lead times of a day or more, such predictions must be made on the basis of remote solar observations. A number of empirical prediction schemes have been proposed to forecast the transit time and speed of coronal mass ejections (CMEs) at 1 AU. However, the current lack of magnetic field measurements in the corona severely limits our ability to forecast the 1 AU magnetic field strengths resulting from interplanetary CMEs (ICMEs). In this study we investigate the relation between the characteristic magnetic field strengths and speeds of both magnetic cloud and noncloud ICMEs at 1 AU. Correlation between field and speed is found to be significant only in the sheath region ahead of magnetic clouds, not within the clouds themselves. The lack of such a relation in the sheaths ahead of noncloud ICMEs is consistent with such ICMEs being skimming encounters of magnetic clouds, though other explanations are also put forward. Linear fits to the radial speed profiles of ejecta reveal that faster-traveling ICMEs are also expanding more at 1 AU. We combine these empirical relations to form a prediction scheme for the magnetic field strength in the sheaths ahead of magnetic clouds and also suggest a method for predicting the radial speed profile through an ICME on the basis of upstream measurements.

Citation: Owens, M. J., P. J. Cargill, C. Pagel, G. L. Siscoe, and N. U. Crooker (2005), Characteristic magnetic field and speed properties of interplanetary coronal mass ejections and their sheath regions, *J. Geophys. Res.*, *110*, A01105, doi:10.1029/2004JA010814.

1. Introduction

[2] The variable solar wind conditions impinging on the Earth's magnetosphere can lead to periods of severe geomagnetic disturbance, commonly referred to as "geomagnetic storms." They can result in adverse effects to a number of space- and ground-based technologies [Feynman and Gabriel, 2000], making prediction of storm onset and severity highly desirable. A major step toward such "space weather" forecasts is the prediction of solar wind conditions in near-Earth space (i.e., at 1 AU). The dusk to dawn electric field (E_Y in GSE coordinates, the product of the solar wind radial flow speed and the southward magnetic field strength) plays a major role in the modulation of magnetic reconnection at the dayside magnetopause and hence controls the rate at which solar

wind energy can be injected into the terrestrial system [Dungey, 1961]. Prediction schemes for "steady state" solar wind conditions have been proposed that use remote solar observations as input (e.g., photospheric field maps [Arge and Pizzo, 2000; Odstrčil et al., 2004]), giving a potential prediction lead time of ~ 3 –5 days. However, prolonged intervals of strong E_Y are often the result of transient structures associated with the interplanetary manifestations of coronal mass ejections (CMEs). Hence prediction of the most severe geomagnetic activity requires prediction of the arrival and properties of interplanetary CMEs (ICMEs) in near-Earth space.

[3] ICMEs at 1 AU typically take of order a day to convect over an observing spacecraft, indicating radial extents of roughly 0.2 AU. They can be identified by a range of in situ signatures, including (but not limited to) low proton temperatures, enhanced field magnitude, high alpha to proton ratio, and bidirectional electron heat flux (see Neugebauer and Goldstein [1997] for references and a

review of ICME signatures). It should be noted that no individual signature is either necessary or sufficient for the identification of an ICME, making classification a somewhat subjective process. A subset of ICMEs, called magnetic clouds, are defined as having a smooth magnetic field rotation (interpreted as a magnetic flux rope) and enhanced magnetic field magnitude coupled with a reduced proton temperature [Burlaga *et al.*, 1981] and comprise somewhere between a third [Gosling, 1990] to a half [Cane and Richardson, 2003] of all ICMEs observed at 1 AU.

[4] ICMEs moving faster than the ambient solar wind will compress and deflect the upstream flow. If the relative speed of the two plasma regimes is greater than the fast-mode wave speed, then a shock will form ahead of the ICME. The region of compressed solar wind bounded by the shock front and the ICME leading edge is referred to as the “sheath.” Magnetic fields in the sheath can frequently be strong enough to cause geomagnetic activity in their own right. Indeed, some quarter [Richardson *et al.*, 2001] to a half [Tsurutani *et al.*, 1988] of all geomagnetic storms can be attributed to ICME sheaths. Despite the geomagnetic importance of sheaths, prediction schemes have previously concentrated on the ICME body, with little attention paid to the compressed solar wind ahead of ejecta.

[5] For ICME and sheath prediction lead times of the order of days, forecasts must be made on the basis of remote observations of CMEs close to the Sun, which are most effectively performed by space-based coronagraphs (e.g., the Large Angle Spectroscopic Coronagraph (LASCO) instrument on board Solar Heliospheric Observatory (SOHO)) [Brueckner *et al.*, 1995]. Earth-directed CMEs often appear as expanding rings or “halos” in coronagraph images due to the expansion of ejecta about the occulting disc [Howard *et al.*, 1982]. Coronagraph-derived speeds of halo events are a measure of the expansion speed of CMEs projected onto the plane of the sky, not the radial propagation speed away from the Sun. Nevertheless, empirical prediction schemes for the arrival times and speeds of ICMEs at 1 AU have been developed that use coronagraph observations of halo CMEs as input [Gopalswamy *et al.*, 2000, 2001; Vršnak and Gopalswamy, 2002]. The remaining parameter crucial for predicting the geomagnetic impact of ejecta is the strength and direction of the magnetic field associated with ICMEs at 1 AU, but advance prediction is severely limited by the lack of magnetic field observations in the corona. This paper offers an indirect prediction scheme for magnetic field strength in the sheaths of ICMEs based upon empirical relationships.

2. Background

[6] The determination of an empirical relationship between the magnetic field intensity and speed of ICMEs at 1 AU could provide a possible means of forecasting their gross magnetic properties. Current understanding of the field-speed correlation in solar wind structures is summarized in this section.

[7] Using observations of 17 previously documented magnetic clouds, Gonzalez *et al.* [1998] found a correlation (linear correlation coefficient, $r_L = 0.71$) between the

maximum magnetic field intensity ($|\mathbf{B}|_{MAX}$) and maximum speed (V_{MAX}), such that

$$|\mathbf{B}|_{MAX}(nT) = 0.047V_{MAX}(\text{km/s}) - 1.1. \quad (1)$$

No such relation was found for “gas driver events” (in this study termed “noncloud ICMEs”). Owens and Cargill [2002] then showed that the $|\mathbf{B}| - V$ relation is not limited to magnetic clouds but holds for all high field intensity regions in the solar wind at 1 AU, with no preselection of transient events. They found a strong correlation ($r_L = 0.83$) between field intensity and speed for all regions of the solar wind in which $|\mathbf{B}|$ exceeded 18 nT for 3 hours or more, such that

$$|\mathbf{B}|_{MAX}(nT) = 0.047V_{MAX}(\text{km/s}) + 0.6. \quad (2)$$

This relation is very similar to that found by Gonzalez *et al.* [1998] for magnetic clouds, however only half of the high $|\mathbf{B}|$ structures could be attributed to magnetic clouds.

[8] In contrast, Owens and Cargill [2004] commented that for a set of 35 ICMEs directly associated with halo CMEs at the Sun 2–5 days earlier, only a weak relation existed between maximum field intensity and speed in the body of the ICMEs. Both magnetic cloud and noncloud ICMEs were included in the study. However, they did report a strong correlation ($r_L = 0.81$) between the maximum magnetic field magnitude ($|\mathbf{B}^{SH}|_{MAX}$) and the maximum speed (V_{MAX}^{SH}) in the sheath region ahead of ICMEs, particularly when the speed relative to the upstream solar wind (V_{SW}) was used:

$$|\mathbf{B}^{SH}|_{MAX}(nT) = 0.080(V_{MAX}^{SH} - V_{SW})(\text{km/s}) + 12.1. \quad (3)$$

The reason for the contrasting results regarding correlations will become clear as we further investigate the speed-field relation. From observations of ~ 200 ICMEs at 1 AU, we select and analyze a subset of ICME observations in which the sheath and ICME boundaries are relatively clear and consider the implications of the results for empirical space weather predictions.

3. Preliminary Analysis

[9] On the basis of in situ magnetic field and plasma measurements, Cane and Richardson [2003] identified 214 ICMEs in the Wind and ACE data sets in the years 1996–2002. They categorized ejecta as magnetic cloud (using the Burlaga *et al.* [1981] definition), cloud-like (exhibiting some degree of smooth field rotation but not fully conforming to the magnetic cloud definition), and noncloud ICMEs (no coherent field rotation). It is worth noting that some of the cloud-like ICMEs do exhibit very smooth magnetic field rotations but fail to qualify for magnetic cloud status due solely to a lack of proton temperature drop; the magnetic field signatures of such ejecta can be still consistent with magnetic flux rope structures. We use the Cane and Richardson [2003] start and end times for both the ICME body and any upstream disturbance (i.e., sheath region) to look for a correlation between magnetic field intensity and speed. Data from the ACE MAG Smith *et al.* [1998] and SWEPAM McComas *et al.* [1998] instruments are used throughout.

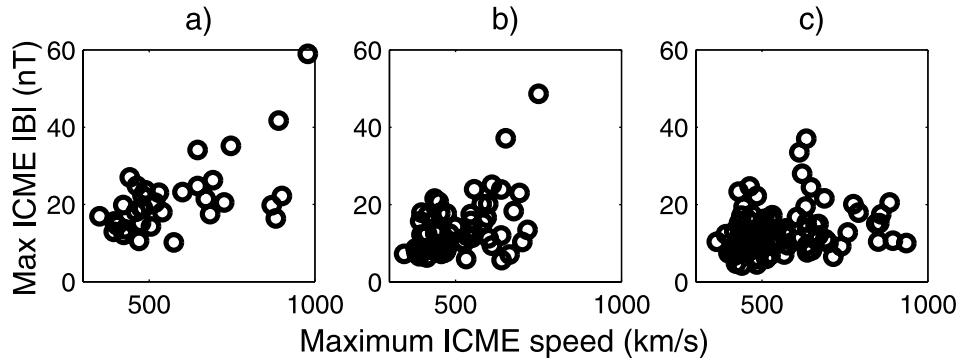


Figure 1. Plots of the maximum speed versus the maximum magnetic field intensity within the body of (a) magnetic cloud, (b) cloud-like, and (c) noncloud interplanetary coronal mass ejections (ICMEs). There is no significant correlation between maximum speed and field intensity for any of the ICME types (see also Table 1).

[10] To enable direct comparison with the results of *Gonzalez et al.* [1998] and *Owens and Cargill* [2002], we first investigate the maximum magnetic field magnitude and the maximum speed in the ICME body. Figure 1 shows these parameters for magnetic cloud (Figure 1a), cloud-like (Figure 1b), and noncloud (Figure 1c) ICMEs. Table 1 lists the best linear fit parameters (of the form $|\mathbf{B}|$ (nT) = mV (km/s) + c) to the $V_{MAX} - |\mathbf{B}|_{MAX}$ scatterplots, along with the associated χ^2 , linear (r_L), and Spearman (r_S) correlation coefficients. In this study, r_S is used to quantify the degree of correlation between two parameters (as it is more statistically robust, greatly reducing the effect of both the distribution of the parameters and any outlying points), whereas r_L is only taken to be a measure of the linearity of any found correlation (see *Owens and Cargill* [2002] for a more detailed discussion of the different correlation coefficients). Visual inspection of Figure 1 and the correlation coefficients in Table 1 suggest rough agreement with the *Gonzalez et al.* [1998] results. There is some correlation between the maximum magnetic field strength and maximum speed in magnetic clouds ($r_S = 0.52$) and essentially none in noncloud ICMEs ($r_S = 0.26$). This agreement disappears, however, with further analysis.

[11] There is a potential problem with using maximum values of magnetic field intensity and speed to characterize an ICME. The declining profile in the radial component of the plasma velocity (i.e., $-V_X$ in GSE coordinates) and the small nonradial components (i.e., V_Y and V_Z) through the

body of a typical ICME (see section 4) means the maximum speed of the ICME body usually occurs at the leading edge. In order to measure this maximum speed, data must be sampled very close to the ICME/sheath boundary, which risks contaminating ICME and sheath observations. However, the flow speed in the sheath region can be higher than in the ICME. Although V_X must approximately balance across the sheath/ICME boundary (the compressed solar wind cannot pass through the ICME leading edge), the sheath can contain significant nonradial flows [e.g., *Owens and Cargill*, 2005] that add to the total speed. Furthermore, sheath regions can also often exhibit higher magnetic field strengths than the ICME body, as shown in Figure 2. Thus maximum $|\mathbf{B}|$ and V values presumably found for the body of an ICME can both inadvertently be sheath measurements instead.

[12] To effectively eliminate small amounts of cross-contamination, this study uses average values to characterize the ICME and sheath magnetic field intensities and speeds. Furthermore, the radial component of the velocity rather than the flow speed is used, although in general the difference between $|V|$ and V_X is negligible except in some highly compressed sheaths. Table 1 summarizes the relation between the average radial speed and the average $|\mathbf{B}|$ in the body of the ICMEs. For these parameters we find no correlation between field and speed in any of the ICME types. In particular, for magnetic clouds, r_S essentially drops to zero.

Table 1. Linear Best Fit Parameters (of the Form $|\mathbf{B}|$ (nT) = mV (km/s) + c) and Correlation Coefficients Between Various Characteristic Interplanetary Coronal Mass Ejections (ICMEs) and Sheath Magnetic Field Intensities and Speeds^a

		ICME Type	m	c	χ^2	r_L	r_S
Maximum speed in ICME body	Maximum $ \mathbf{B} $ in	noncloud	0.010	7.40	0.031	0.227	0.257
		cloud-like	0.035	-4.01	0.025	0.472	0.374
	ICME body	cloud	0.034	2.15	0.023	0.606	0.516
Average V_X in ICME body	Average $ \mathbf{B} $ in	noncloud	0.001	7.49	0.029	0.038	0.103
		cloud-like	0.021	-0.29	0.029	0.320	0.143
	ICME body	cloud	0.005	10.1	0.058	0.160	-0.013
Average V_X in sheath	Average $ \mathbf{B} $ in	noncloud	0.015	3.61	0.041	0.331	0.369
		cloud-like	0.038	-6.18	0.023	0.502	0.429
	sheath	cloud	0.040	-5.76	0.038	0.695	0.645

^aApproximately 200 ICMEs (taken from the *Cane and Richardson* [2003] list) are considered. The relation appears strongest in the sheath region ahead of magnetic clouds.

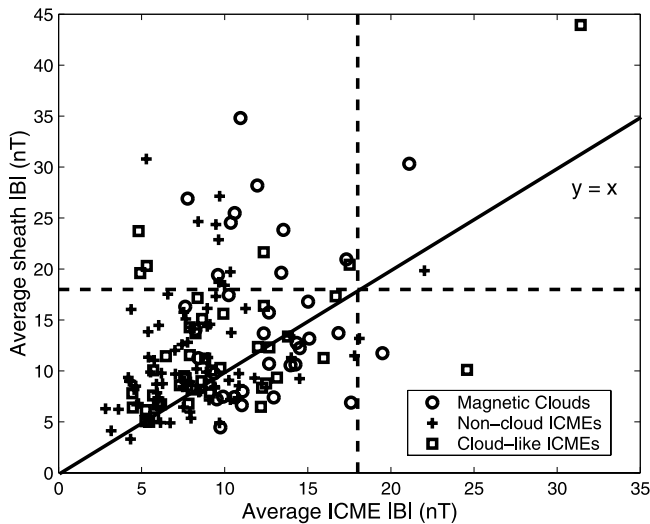


Figure 2. The average $|B|$ in the body of an ICME against that in the preceding sheath region. The various classes of ICME are indicated. There is no obvious relation between the sheath and ICME body magnetic field strengths for any of the ICME types. Note that in general the magnetic field intensity in the sheath is as high if not higher than that of the associated ICME body. Dashed lines show the 18nT events threshold used by Owens and Cargill [2002]. The sheath $|B|$ is higher than the ICME $|B|$ in 89% of such events.

[13] Table 1 also summarizes the relation between the average sheath magnetic field intensity ($|B|_{AVG}^{SH}$) and average sheath radial speed ($V_{X,AVG}^{SH}$) for the three types of ICME. There is a reasonable level of correlation between field and speed in the sheaths ahead of magnetic clouds. We suggest that this relation is responsible for the results of Gonzalez *et al.* [1998], as it is likely that some sheath region was included when the ICME boundaries were chosen and hence may have influenced the maximum ICME properties. Owens and Cargill [2002] defined their events as regions of the solar wind with high field intensities and therefore included a high proportion of sheaths (see Figure 2). In the next section we investigate the relation between average magnetic field intensity and speed in greater detail and suggest possible applications to space weather prediction.

4. Detailed Analysis

[14] From the Cane and Richardson [2003] list we selected a subset of ICMEs with relatively clear sheath and ICME boundaries. The start of the sheath region is simply defined as the arrival of an interplanetary shock ahead of an ICME. However, the start and end of an ICME body are more difficult to precisely define, as a single ICME signature is often insufficient for identification and different ICME signatures rarely “switch on” simultaneously [Neugebauer and Goldstein, 1997]. Thus we use the colocated onset or cessation of two or more ICME signatures as a working definition for the ICME boundaries. The start of a coherent magnetic structure is particularly useful for identifying the ICME leading edge, as the sheath often contains highly variable magnetic fields resulting from the faster ICME “sweeping up” and com-

pressing preexisting structures in the solar wind. This necessarily lends a selection bias toward magnetic cloud ICMEs. In addition to the signatures traditionally employed in ICME identification (i.e., those listed in section 1), we also found the three-dimensional velocity data to be useful in differentiating between sheath and ICME plasma. Nonradial components of the plasma flow velocity (V_Y and V_Z in GSE coordinates) are distinguishing characteristics of sheaths, where the ambient flow is deflected around the ICME leading edge [e.g., Owens and Cargill, 2005]. The ICME body frequently exhibits a smoothly declining profile in the radial component of the flow velocity (V_X in GSE coordinates), owing to expansion (e.g., see Figure 3 and section 6).

[15] Proceeding in this manner we selected 62 ICMEs for use in this study: 30 were classified as magnetic clouds by Cane and Richardson [2003], 16 were classified as non-cloud ICMEs, and 16 were classified as cloud-like events. Of the 62 events, 50 were driving shocks and hence had clear sheath regions.

[16] To objectively characterize the 1 AU speeds of ejecta, we perform linear fits to the V_X time series through the ICME bodies and use the fit parameters to define characteristic speeds of the ICME, as shown in Figure 3. By using the fit parameters rather than taking the values directly from the in situ data, the effect of small-scale speed fluctuations and local variations is greatly reduced, while the large-scale dynamics of the ICME is captured. Furthermore, this method reduces the impact of any data gaps. We include only ICMEs in which the linear fit is deemed adequate to describe the radial speed profile ($\chi^2 < 0.01$), reducing the number of ICMEs considered from 50 to 37.

[17] Characteristic ICME speeds are now defined as follows (see also Figure 3). The cruise speed (V_{CR}) of an ICME is taken to be the radial speed at the midpoint of the ejecta. Thus V_{CR} is the bulk speed of the ICME at 1 AU and,

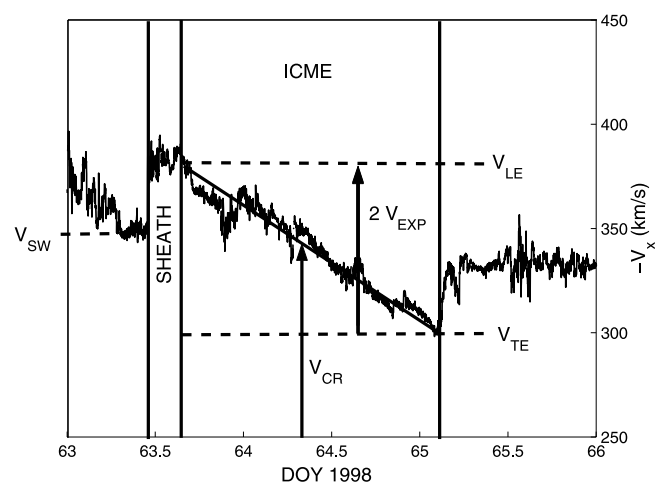


Figure 3. A linear fit to the radial speed time series through the body of an ICME is used to define a number of characteristic speeds. The cruise speed (V_{CR}) is the speed at the midpoint of the ICME body; the leading (V_{LE}) and trailing edge (V_{TE}) speeds are the speeds at the front and rear ICME boundaries. The expansion speed (V_{EXP}) is then defined as half the difference between V_{LE} and V_{TE} .

Table 2. Linear Best Fit Parameters (of the Form $|\mathbf{B}|$ (nT) = mV (km/s) + c) and Correlation Coefficients Between Various Characteristic ICME Magnetic Field Intensities and Speeds for the 37 ICMEs With Well-Defined Boundaries and Speed Profiles^a

		ICME Type	m	c	χ^2	r_L	r_S
Maximum speed in ICME body ($\sim V_{LE}$)	Maximum	noncloud	-0.011	4.66	0.092	-0.434	-0.436
	$ \mathbf{B} $ in	cloud-like	0.012	18.5	0.153	0.235	0.107
Average V_X in ICME body ($\sim V_{CR}$)	ICME body	cloud	-0.032	-0.140	0.041	-0.523	-0.239
	Average	noncloud	0.012	1.73	0.067	0.425	0.418
Average V_X in sheath	$ \mathbf{B} $ in	cloud-like	-0.017	16.0	0.130	-0.242	-0.536
	ICME body	cloud	0.030	-1.79	0.032	0.526	-0.061
	Average	noncloud	0.007	8.20	0.079	0.289	0.164
	$ \mathbf{B} $ in	cloud-like	-0.052	45.4	0.140	-0.490	-0.500
ICME leading edge V_X - upstream V_{SW}	sheath	cloud	0.039	-6.27	0.044	0.767	0.748
	Average	noncloud	-0.005	13.8	0.085	-0.152	-0.200
	$ \mathbf{B} $ in	cloud-like	0.108	-2.71	0.060	0.823	0.900
	sheath	cloud	0.049	6.43	0.016	0.899	0.892

^aThe relation is strongest between the magnetic field intensity in the sheath region ahead of magnetic clouds and the leading edge speed in the upstream solar wind frame.

in general, is approximately equal to the radial speed averaged over the whole ICME body. The leading edge speed (V_{LE}) is the radial speed of the linear fit at the leading ICME boundary and hence normally corresponds to the maximum speed of the ICME. The trailing edge speed (V_{TE}) is defined in a similar manner and is the minimum speed for most ejecta. An ICME expansion speed (V_{EXP}) can then be defined as half the difference between the speeds at the leading and trailing edges:

$$V_{EXP} = (V_{LE} - V_{TE})/2. \quad (4)$$

The rate of radial expansion is simply the gradient of the linear fit (m_{EXP}). Last, the upstream solar wind speed (V_{SW}) is defined as the 0.2 day average of V_X ahead of the shock front.

[18] Table 2 shows the same relations between average magnetic field intensity and speed considered in the preliminary analysis but for the subset of ICMEs with well-defined boundaries. The correlation between magnetic field intensity and speed is highest in the sheath region ahead of magnetic clouds. Since sheath regions are the result of ambient solar wind compression resulting from a fast-moving ICME sweeping up material ahead of it, the degree of compression in the sheath (and therefore the magnetic field intensity) should be controlled by the radial speed of the ICME leading edge relative to the upstream solar wind, i.e., $V_{LE} - V_{SW}$. Figure 4 shows how $V_{LE} - V_{SW}$ correlates with $|\mathbf{B}^{SH}|_{AVG}$ for the three classes of ICME. The best linear fit parameters and correlation coefficients are listed in Table 2. Magnetic clouds exhibit a strong correlation between these two parameters (linear correlation = 0.90, Spearman correlation = 0.89) such that

$$|\mathbf{B}^{SH}|(nT) = 0.049(V_{LE} - V_{SW})(\text{km/s}) + 6.43nT. \quad (5)$$

The gradient of this relation is similar to the previously reported maximum field intensity and speed relations (equations (1) and (2)). However, the y-axis intercept is much higher because the upstream solar wind speed has been subtracted. Note that as the leading edge speed in the solar wind frame tends toward zero, the sheath field intensity tends toward typical ambient solar wind values.

[19] Noncloud ICMEs do not show any correlation between sheath field intensity and ICME leading edge speed in the solar wind frame, though there are insufficient observations to definitively rule it out. Worth noting is the existence of noncloud ICMEs with high speeds (in the solar wind frame) and low sheath magnetic field strengths. For the cloud-like ICMEs, the few data points available seem to follow the same trend as the magnetic cloud events.

[20] The derived empirical relation between sheath field intensity and speed relative to the solar wind (equation (5)) provides a way to predict the gross magnetic properties of the disturbed solar wind ahead of ejecta, which can be extremely geoeffective. Such a prediction scheme is considered in the next section.

5. Predicting Sheath Fields

[21] With the empirical relations outlined in the previous section, the magnitude of the sheath magnetic field can be predicted if the speed of the ICME leading edge is known relative to the ambient solar wind speed, at least for magnetic clouds. The ambient solar wind speed at 1 AU can be predicted by empirical models such as the Wang-Sheeley-Argé model (WSA) [Argé and Pizzo, 2000] or by coupled MHD models of the corona and heliosphere [Odstrčil et al., 2004]. Though such models cannot yet include transient events on a routine basis, predictions of the ambient solar wind conditions are still possible at periods close to the actual ejecta [Argé et al., 2004]. Empirical models of ICME 1 AU travel times [e.g., Gopalswamy et al., 2001; Vršnak and Gopalswamy, 2002] can also predict the 1 AU cruise speeds of ICMEs. We will proceed assuming these two parameters are known. Testing their prediction accuracy is beyond the scope of this study. Readers are instead referred to Argé and Pizzo [2000] and Owens and Cargill [2004].

[22] The empirical relation in equation (5) allows a prediction of average sheath field intensity using the ICME leading edge speed. Thus we need to relate the cruise speed (V_{CR} , provided by the ICME transit models) to the leading edge speed (V_{LE}) of ICMEs. Figure 5 shows the ICME leading edge speed as a function of cruise speed for the three classes of ICME. For slower ICMEs there is little difference between these two char-

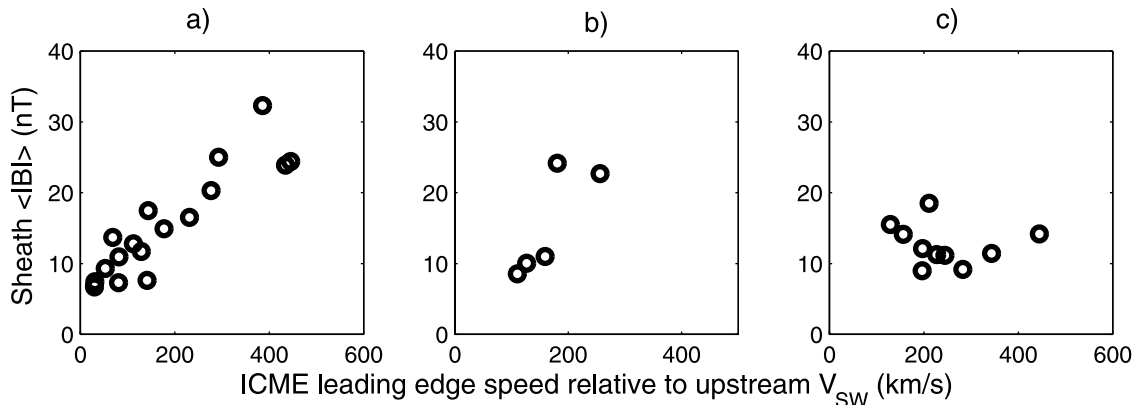


Figure 4. Plots of the ICME leading edge speed (relative to the upstream the solar wind) versus the average magnetic field intensity in the sheath for (a) magnetic clouds, (b) cloud-like ICMEs, and (c) noncloud ICMEs. There is strong correlation for magnetic clouds. However, further observations are required for cloud-like and noncloud ICMEs.

acteristic speeds; however, for faster-traveling ICMEs this difference can be >100 km/s, which can have a significant impact on the predicted sheath field strength and thus needs to be taken into account. Note that the difference between the leading edge and cruise speed increases steadily with increasing cruise speed, suggesting that fast traveling ICMEs are also expanding more at 1 AU (see also section 6).

[23] We find the best linear fit between the leading edge and cruise speeds of ICMEs to be

$$V_{LE}(\text{km/s}) = (1.30V_{CR} - 57.7)\text{km/s}. \quad (6)$$

Thus the sheath field magnitude can be predicted by combining the empirical relations between V_{LE} and V_{CR} and $|\mathbf{B}^{SH}|$ and $(V_{LE} - V_{SW})$, such that

$$|\mathbf{B}^{SH}|_{\text{PRED}}(\text{nT}) = 0.049[1.30V_{CR} - (V_{SW} + 57.7)] + 6.43\text{nT}. \quad (7)$$

Using observed values for the upstream solar wind and ICME cruise speed, the average error between the observed sheath field intensity and that calculated using equation (7) is 2.4 nT (7.5 nT) for magnetic cloud (all) ICMEs at 1 AU, giving a potential prediction accuracy of 86% (56%). Figure 6 shows the calculated versus observed sheath field magnitude.

[24] As can be seen from Figure 6, reasonable predictions of the average sheath magnetic field intensity can potentially be made for magnetic cloud and cloud-like ICMEs (assuming the upstream solar wind and 1 AU ICME cruise speeds are known). However, such intensities predicted for noncloud ICMEs are generally much higher than those observed. Section 7 discusses a possible explanation of this effect. In the next section we outline empirical relations between the characteristic ICME speeds and suggest possible applications to space weather prediction.

6. ICME Speed Characteristics

[25] We now introduce a new empirical relation involving the characteristic speeds of ICMEs at 1 AU (as defined in section 4 and Figure 3). Figure 7a shows how the leading

edge (V_{LE}) and expansion (V_{EXP}) speeds of ICMEs are linearly related. (Note that due to the strong correlation between V_{LE} and V_{CR} , we also find a similarly strong relation between V_{CR} and V_{EXP} . We detail the $V_{LE}-V_{EXP}$ relation here, as it most useful for a potential prediction scheme outlined at the end of this section.) For all ICME types,

$$V_{EXP}(\text{km/s}) = 0.266V_{LE} - 70.6\text{km/s}. \quad (8)$$

Thus faster ejecta (both magnetic cloud and noncloud ICMEs) are also expanding faster at 1 AU. This relation has a linear (Spearman) correlation coefficient of 0.84 (0.88). Discussion of this phenomenon is provided in section 7.

[26] A second (similar) relation exists between m_{EXP} (the gradient of the V_X time series) and the leading edge speed, (Figure 7b): m_{EXP} also increases with ICME speed. Note that m_{EXP} is the value of dV_X/dt averaged over the ICME

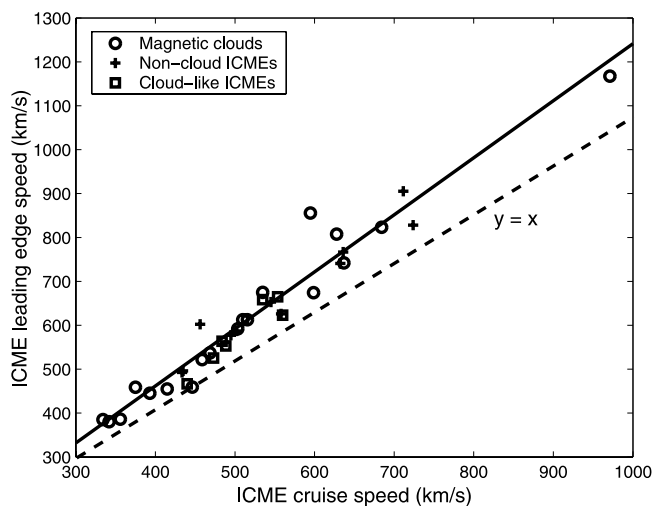


Figure 5. The relation between the cruise speed of ICMEs to the leading edge speed. The line of best fit to the magnetic cloud events ($V_{LE}(\text{km/s}) = 1.30V_{CR} - 57.7\text{km/s}$) is shown as the solid line (it is essentially identical to the fit to the all ICMEs) and can be used to infer the leading edge speed from the cruise speed.

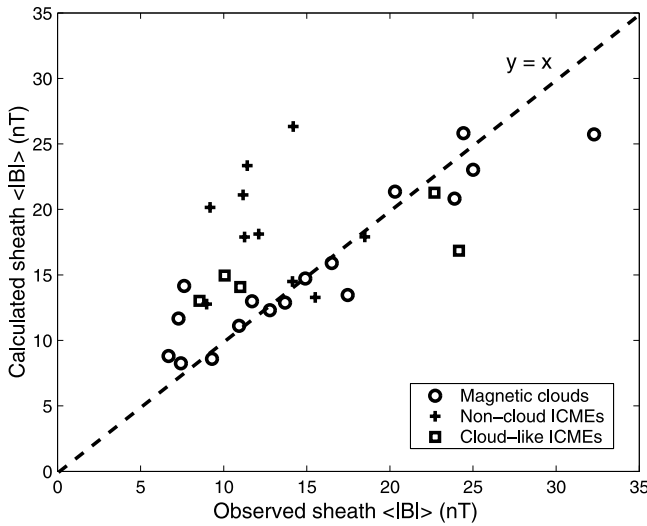


Figure 6. The empirically calculated average sheath magnetic field intensity (using the observed values of the upstream solar wind speed and ICME cruise speed) as a function of observed average sheath field intensity. Reasonable accuracy is achieved for magnetic cloud and cloud-like ICMEs, but the sheath field intensities are generally overestimated for noncloud ICMEs.

body and hence is the expansion rate of the ICME at 1 AU. A quadratic fit is more appropriate than a linear fit:

$$m_{EXP} = 10^{-8}(1.19V_{LE}^2 - 954V_{LE} + 284180)\text{km/s}^2. \quad (9)$$

This is also a strong relation, with a Spearman correlation coefficient of 0.88. By combining equations (8) and (9), the radial speed time series through the body of an ICME can be prescribed for a given leading edge speed. We note that the *Gopalswamy et al.* [2000] relation between the speed of ejecta at the Sun and Earth and the expansion speed relation of equation (8) are consistent with ICMEs at 1 AU having widths ~ 0.2 AU. However, the *Gopalswamy et al.* [2000]

relation and the expansion rate relation of equation (9) give ICME widths both much smaller and larger than those observed at 1 AU. This suggests that while the expansion speed of ejecta remains fairly constant during the transit from the Sun to the Earth, the rate of expansion does not. Further study of these relations is required. The remainder of this section outlines a possible application to space weather forecasting.

[27] Many space weather prediction schemes can be split into two distinct classes: accurate but short lead-time (~ 30 min) predictions based upon in situ L1 observations, or advanced but often less accurate forecasts based upon remote solar or coronal observations (giving \sim days lead time). *Chen et al.* [1997] suggested a “hybrid” scheme yielding intermediate lead times: L1 measurements of the leading portion of a magnetic cloud are used to infer the magnetic field structure of the rest of the cloud further downstream. This method harnesses the accuracy of using in situ measurements but also gives extended lead times between ~ 30 min (the front of the cloud) and \sim day (the rear of the cloud).

[28] We propose a similar, complimentary scheme for predicting the radial speed profile through the ICME body. Equation (5) predicts the leading edge speed of ICMEs on the basis of the upstream solar wind speed and the average sheath magnetic field magnitude. Equation (8) predicts the total change in radial speed over the ICME body from the leading edge speed, which, coupled with the rate of change of radial speed (from equation (9)), allows an estimate of the ICME duration and, more importantly, a prediction of the radial speed profile throughout the body of the ICME. Both the input parameters (V_{SW} and $|\mathbf{B}^{SH}|$) can be measured while an observing spacecraft (e.g., at L1) is in the sheath region, upstream of the actual ICME. As shocks typically stand ~ 0.25 to 0.5 days upstream of the ICME leading edge [*Russell and Mulligan, 2002*], observations made in the sheath could (in principle) be used to predict properties of the driving ICME with lead times ranging from ~ 0.25 (front) to 1.5 days (rear of an ICME).

[29] Using a *Chen et al.* [1997] forecast of the southward magnetic field component through a magnetic cloud in

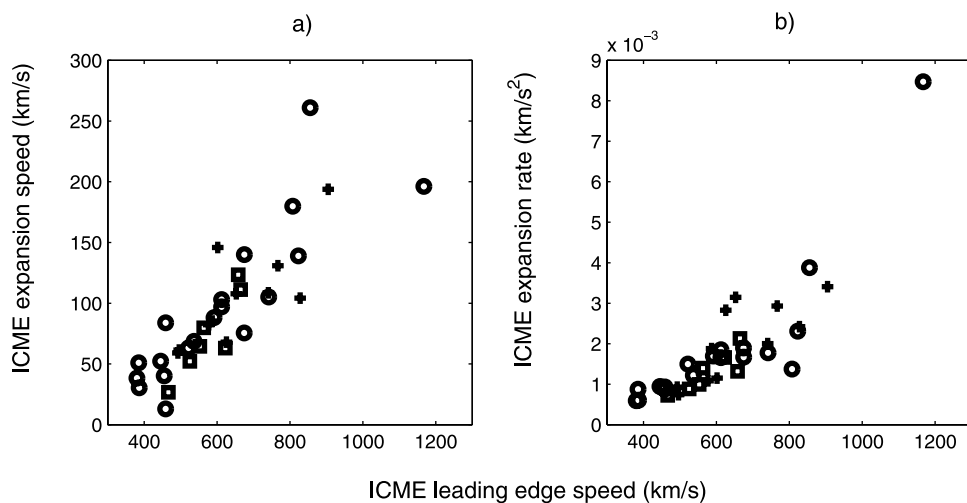


Figure 7. The (a) expansion speed and (b) rate as a function of ICME leading edge speed. Magnetic clouds, cloud-like, and noncloud ICMEs are represented as circles, squares, and crosses, respectively. For all ICME types, faster traveling ejecta are expanding more at 1 AU.

conjunction with our radial speed prediction would allow prediction of the dawn-to-dusk electric field, the key factor in the rate of dayside reconnection at the magnetopause. However, the validity and accuracy of such a scheme has yet to be tested.

7. Discussion and Conclusions

[30] Using both a survey of a large number of ICMEs and a detailed analysis of a carefully selected subset of ejecta, we conclude that the previously reported correlation between the magnetic field strength and speed of ICMEs at 1 AU is the result of ambient solar wind compression in the sheath region ahead of ejecta rather than an intrinsic property of magnetic clouds. Correlation is strongest between sheath field intensity and ICME leading edge speed in the solar wind reference frame for ICMEs displaying the signatures of a magnetic cloud (most notably a smooth rotation in the magnetic field direction). Noncloud ICMEs display a much lower level of correlation between sheath field intensity and leading edge speed, mainly due to a large number of fast noncloud ICMEs with low sheath field intensities. These events could be the result of spacecraft encounters with magnetic clouds that merely skim the edge of the flux rope: such an encounter might miss the smooth field rotation, and the ICME would thus be classified as a noncloud event. Furthermore, the skimming trajectory would intercept the shock front away from the nose, where the stand-off distance is greater and hence the sheath is less compressed [e.g., Owens and Cargill, 2005]. On the basis of this result we suggest many noncloud ICMEs may have a flux rope structure that is not observed due to the trajectory of the spacecraft through the ejecta. MHD simulations of ICMEs seem to be consistent with this idea [e.g., Riley et al., 2004]. Alternatively, the difference in sheath compression between magnetic cloud and noncloud ICMEs could also be explained in terms of two morphologically different types of ejecta [Russell and Mulligan, 2002]. Multispacecraft measurements of the same ejecta at large separations are required to resolve this issue.

[31] A linear fit to the declining radial speed profile through the body of the ejecta is adequate to describe a large fraction ($\sim 75\%$) of the ICMEs catalogued by Cane and Richardson [2003], at least when the boundaries can be readily identified. On the basis of linear fits to the radial speed profiles, the expansion speed of an ICME at 1 AU is found to be linearly related to its cruise speed for both magnetic cloud and noncloud ICMEs. This might be expected, as fast ICMEs should move away from slower solar wind behind them, creating a rarefaction wave that propagates into the ICME and results in expansion. However, it seems that the radial expansion is at least to some degree internally driven, as frequently the trailing edge of the ICME is moving significantly slower than the solar wind immediately behind it (e.g., see Figure 3). ICMEs with a higher internal pressure are expected to expand more [e.g., Gosling et al., 1998] and it is possible that such ejecta would also be decelerated less by the aerodynamic drag of the solar wind [e.g., Cargill, 2004]. Other explanations could relate to the details of CME initiation, with a radial speed gradient being in some way intrinsic to the launch mechanism. A more detailed investigation of ICME expansion,

with comparison to MHD or numerical models, may lead to better understanding of the nature of this relation.

[32] This study has also considered the feasibility of using these empirical relations to make long lead time (\sim days) forecasts of the geoeffectiveness of ejecta. It had previously been suggested that the relation between magnetic field strength and speed could be used to predict the gross magnetic properties of ICMEs [e.g., Gonzalez et al., 1998; Owens and Cargill, 2002]. However, in the ICME body we find no significant correlation between these parameters, negating its usefulness as an empirical prediction tool. Instead, we propose two new empirical prediction schemes that utilize the speed-field relation in the sheath ahead of ICMEs. The most obvious use is to forecast the sheath field intensity on the basis the ICME cruise speed (which can be estimated by ICME transit models taking coronagraph observations of halo CMEs as input), giving a potential forecast lead time of \sim days. Such a prediction scheme would be a useful space weather tool, as the sheaths ahead of ICMEs can often be as geoeffective as the ICMEs themselves.

[33] The second possible application of the sheath field-speed relation is in predicting the speed profile of the ICME body, while the in situ observing spacecraft is still located in the preceding sheath. Direct measurements of the upstream solar wind speed and the sheath field magnitude can be used to predict both the ICME radial speed profile and ICME duration. This method could be used in conjunction with that of Chen et al. [1997] to provide a time series of the dawn-to-dusk electric field, with up to a day lead time.

[34] **Acknowledgments.** This research was supported by the National Science Foundation under agreement ATM-012950 (M.O. and G.S.), which funds the CISM project of the STC program and under grant ATM-0119700 (N.C.). We have benefited from the availability of ACE data at NSSDC, in particular the MAG (P.I. N. Ness) and SWEPAM (P.I. D. McComas) instruments.

[35] Shadia Rifai Habbal thanks Vasyliadis Yurchyshyn and Walter D. Gonzalez for their assistance in evaluating this paper.

References

- Arge, C. N., and V. J. Pizzo (2000), Improvement in the prediction of solar wind conditions using near-real time solar magnetic field updates, *J. Geophys. Res.*, *105*, 10,465.
- Arge, C. N., J. Luhmann, D. Odstrčil, C. J. Schrijver, and Y. Li (2004), Stream structure and coronal sources of the solar wind during the May 12, 1997 CME, *J. Atmos. Sol. Terr. Phys.*, in press.
- Brueckner, G. E., et al. (1995), The large angle spectroscopic coronagraph (LASCO), *Sol. Phys.*, *162*, 357.
- Burlaga, L. F., E. Sittler, F. Mariani, and R. Schwenn (1981), Magnetic loop behind and interplanetary shock: Voyager, Helios, and IMP 8 observations, *J. Geophys. Res.*, *86*, 6673–6684.
- Cane, H. V., and I. G. Richardson (2003), Interplanetary coronal mass ejections in the near-Earth solar wind during 1996–2002, *J. Geophys. Res.*, *108*(A4), 1156, doi:10.1029/2002JA009817.
- Cargill, P. J. (2004), On the aerodynamic drag force acting on coronal mass ejections, *Solar Phys.*, *221*, 135.
- Chen, J., P. J. Cargill, and P. J. Palmadesso (1997), Predicting solar wind structures and their geoeffectiveness, *J. Geophys. Res.*, *102*, 14,701.
- Dungey, J. W. (1961), Interplanetary magnetic field and the auroral zones, *Phys. Rev. Lett.*, *6*, 47.
- Feynman, J., and S. B. Gabriel (2000), On space weather consequences and predictions, *J. Geophys. Res.*, *105*, 10,543.
- Gonzalez, W. D., A. L. Clua De Gonzalez, A. Dal Lago, B. T. Tsurutani, J. K. Arballo, G. S. Lakhina, B. Buti, and G. M. Ho (1998), Magnetic cloud field intensities and solar wind velocities, *Geophys. Res. Lett.*, *25*, 963.
- Gopalaswamy, N., A. Lara, R. P. Lepping, M. L. Kaiser, D. Berdichevsky, and O. C. St. Cyr (2000), Interplanetary acceleration of coronal mass ejections, *Geophys. Res. Lett.*, *27*, 145.

- Gopalswamy, N., A. Lara, S. Yashiro, M. L. Kaiser, and R. A. Howard (2001), Predicting the 1-AU arrival times of coronal mass ejections, *J. Geophys. Res.*, *106*, 29,207.
- Gosling, J. T. (1990), Coronal mass ejections and magnetic flux ropes in interplanetary space, in *Physics of Magnetic Flux Ropes*, *Geophys. Monogr. Ser.*, vol. 58, edited by E. R. Priest, L. C. Lee, and C. T. Russell, pp. 343–364, AGU, Washington, D. C.
- Gosling, J. T., P. Riley, D. J. McComas, and V. J. Pizzo (1998), Overexpanding coronal mass ejections at high heliographic latitudes: Observations and simulations, *J. Geophys. Res.*, *103*, 1941.
- Howard, R. A., D. J. Michels, N. R. Sheely, and M. J. Koomen (1982), The observation of a coronal transient directed at Earth, *Astrophys. J. Lett.*, *263*, 101.
- McComas, D. J., S. J. Bame, S. J. Barker, W. C. Feldman, J. L. Phillips, P. Riley, and J. W. Griffee (1998), Solar wind electron proton alpha monitor (SWEPAM) for the Advanced Composition Explorer, *Space Sci. Rev.*, *86*, 563.
- Neugebauer, M., and R. Goldstein (1997), Particle and field signatures of coronal mass ejections in the solar wind, in *Coronal Mass Ejections*, *Geophys. Monogr. Ser.*, vol. 99, edited by N. Crooker, J. A. Joselyn, and J. Feynman, p. 245, AGU, Washington, D. C.
- Odstrčil, D., V. Pizzo, J. A. Linker, P. Riley, R. Lionello, and Z. Mikic (2004), Initial coupling of coronal and heliospheric numerical magneto-hydrodynamic codes, *J. Atmos. Sol. Terr. Phys.*, *66*, 1311.
- Owens, M. J., and P. J. Cargill (2002), Correlation of magnetic field intensities and solar wind speeds of events observed by ACE, *J. Geophys. Res.*, *107*(A5), 1050, doi:10.1029/2001JA000238.
- Owens, M. J., and P. J. Cargill (2004), Predictions of the arrival time of Coronal Mass Ejections at 1 AU: An analysis of the causes of errors, *Ann. Geophys.*, *22*, 661.
- Owens, M. J., and P. J. Cargill (2005), Non-radial solar wind flows induced by the motion of interplanetary coronal mass ejections, *Ann. Geophys.*, in press.
- Richardson, I. G., E. W. Cliver, and H. V. Cane (2001), Sources of geomagnetic storms during nearly three solar cycles (1972–2000), *Geophys. Res. Lett.*, *28*, 2569.
- Riley, P., J. A. Linker, R. Lionello, Z. Mikic, D. Odstrčil, M. A. Hidalgo, Q. Hu, R. P. Lepping, B. J. Lynch, and A. Rees (2004), Fitting flux-ropes to a global MHD solution: A comparison of techniques, *J. Atmos. Sol. Terr. Phys.*, *66*, 1321.
- Russell, C. T., and T. Mulligan (2002), On the magnetosheath thicknesses of interplanetary coronal mass ejections, *Planet. Space Sci.*, *50*, 527.
- Smith, C. W., J. L'Heureux, N. F. Ness, M. H. Acuna, L. F. Burlaga, and J. Scheifele (1998), The ACE magnetic fields experiment, *Space Sci. Rev.*, *86*, 613.
- Tsurutani, B. T., W. D. Gonzalez, F. Tang, S. I. Akasofu, and E. J. Smith (1988), Origin of the interplanetary southward magnetic fields responsible for the major magnetic storms near solar maximum (1978–1979), *J. Geophys. Res.*, *93*, 8519.
- Vršnak, B., and N. Gopalswamy (2002), Influence of aerodynamic drag on the motion of interplanetary ejecta, *J. Geophys. Res.*, *107*(A2), 1019, doi:10.1029/2001JA000120.

P. J. Cargill, Space and Atmospheric Physics, The Blackett Laboratory, Imperial College, London SW7 2BZ, UK.

N. U. Crooker, M. J. Owens, C. Pagel, and G. L. Siscoe, Center for Space Physics, Boston University, Boston, MA 02215, USA. (mjowens@bu.edu.)